PERGAMON

Journal of Structural Geology 22 (2000) 1437–1454

JOURNAL OF STRUCTURAL GEOLOGY

www.elsevier.nl/locate/jstrugeo

Intrusion within a transtensional tectonic domain: the Čistá granodiorite (Bohemian Massif)—structure and rheological modelling

Zdeněk Venera [a], Karel Schulmann [a], Alfred Kröner [b]

[a] *Institute of Petrology and Structural Geology, Faculty of Science, Universita Karlova, Albertov 6, Prague 128 43, Czech Republic*
[b] *Institut für Geowissenschaften, Universität Mainz, 55099 Mainz, Germany*

Received 2 December 1998; accepted 23 April 2000

Abstract

The Čistá granodiorite stock, which intrudes the Tis granite laccolith, and their Neoproterozoic country rocks of the Teplá–Barrandian zone were studied by means of structural analysis and anisotropy of magnetic susceptibility. The rocks were dated by the Pb–Pb evaporation on zircons, determining the age of the Čistá granodiorite and Tis granite at 373 Ma and 504 Ma, respectively. The structures in the country rocks are characterised by an axial cleavage dipping to the northwest and overprinting the folded bedding. S_1 cleavage bears NE–SW-trending mineral lineations, which plunge to the northeast or southwest at shallow angles. The cleavage is deformed by D_2 kink-bands, which indicate a vertical shortening and a NW–SE stretching. Both the Čistá granodiorite stock and the Tis granite are deformed by a sinistral transtensional shear zone. The geometry of this zone is compatible with the D_2 brittle-ductile extensional kink-bands developed in the metasediments. According to microstructures in the granitoids affected by the shear zone, we show that the Tis granite was deformed in solid-state at high temperatures, whilst the Čistá granodiorite developed both the magmatic and high-temperature solid-state deformation fabric during its syntectonic cooling. Numerical thermal and rheological modelling of the Čistá granodiorite intrusion suggests that it caused an important weakening of the crust at the site of emplacement, which in combination with regional transtension explains that it became the site of a ductile shear zone.

1. Introduction

Magma ascent and emplacement in the crust occur in various deformation regimes which can be tentatively deduced from a structural study around the intrusion (Brun and Pons, 1981; Vigneresse, 1995a). An important factor controlling the emplacement of a pluton and its microstructural evolution, which is in turn related to the rate of magma cooling, is the depth of magma emplacement (Vigneresse, 1995b).

This work deals with the structural relationships between a Variscan granodiorite pluton emplaced at a shallow crustal level, an early Palaeozoic (Caledonian) laccolith and the low-grade Neoproterozoic country rocks. We demonstrate that the granodiorite stock was emplaced along a strongly localised ductile transtensional shear zone cross-cutting the granite laccolith. We correlate this shear zone affecting both granitoids with regionally distributed extensional deformation affecting the Neoproterozoic metasediment previously subjected to compression. An important objective of this study is understanding the strain localisation within the granodiorite stock during its intrusion into the previously undeformed granite laccolith.

We present results of mesoscopic structural analysis of polyphase deformation carried out in both the country rocks and in the granodiorite intrusion. We accomplish this by a detailed anisotropy of magnetic susceptibility (AMS) study in igneous rocks, and by microstructural and microfabric analyses of the deformed granitoids. A combination of mesoscopic structural study, AMS and microstructural analysis enables us to recognise the transtensional mode of granodiorite emplacement and to distinguish whether

0191-8141/00/$ - see front matter
PII: S0191-8141(00)00054-7

the studied fabric resulted from magmatic flow, progressive solidification during syntectonic magma cooling and emplacement, or solid-state deformation superimposed on solidified rocks. This approach allowed us to evaluate: (i) the fabric evolution from the magmatic stage to the ultramylonite solid-state in the granodiorite stock, and (ii) the effect of superimposition of magmatic heat supplied by the granodiorite onto the fossil magmatic fabric of the already solidified granite laccolith.

We use the geological model developed here as a base for thermal and rheological modelling to explain weakening of a rigid granite sheet by ascending granodiorite magma and activation of localised ductile shear zone in a regional extensional regime. The microstructural analysis is further used to explain the localisation of deformation in both the progressively cooled granodiorite and syntectonically heated solid granite. The mechanical evolution of the two types of rocks is modelled using rheological modelling of polyphase tectonites in a transient thermal regime.

2. Geological setting

The study area is located in the north-western flank of the Teplá–Barrandian zone in the Bohemian Massif (Fig. 1). The central part of the Teplá–Barrandian is composed of two stratigraphic sections which differ in structural style. Unmetamorphosed Ordovician to Middle Devonian sediment is folded with NE–SW-trending fold hinges and affected by several NW- or SE-dipping thrusts. They lie unconformably on weakly metamorphosed anchizonal Neoproterozoic and Cambrian volcano-sedimentary rocks (Dudek and Fediuk, 1955; Chlupáč, 1993). Locally the Teplá–Barrandian was intruded by basalt and granitoid porphyry dykes striking NE–SW, and by granitic to gabbroic intrusions of Cambro-Ordovician age (Zulauf, 1997). The latter rocks exhibiting a different structural style and are thought to have undergone a pre-Variscan deformation (Holubec, 1973). However, new structural studies show folding of Neoproterozoic strata and development of steep crenulation cleavage in the central part of the Teplá–Barrandian (Zulauf, 1997). To the northwest, a transition to thrust related higher-grade metamorphic foliation, dipping at shallow angles to the SE, is observed.

To the west of the Barrandian Palaeozoic, the metamorphic grade of the central part of the Neoproterozoic rocks increases westwards from anchimetamorphic slates and graywackes through NE–SW-trending chlorite, biotite, garnet, and staurolite zones, towards a kyanite zone at the western contact with the Moldanubian (Cháb et al., 1995; Zulauf, 1997). Pressures of 6–7 kbar and temperatures of 500–550°C were estimated for the garnet zone and 8 kbar at 580°C for the staurolite zone (Zulauf, 1997). Pressure–temperature conditions of 5–9 kbar and 580–640°C were estimated for the kyanite zone by Cháb and Žáček (1994). Zulauf (1999) correlated the increasing metamorphic grade with the general character of Variscan compressive deformation, which is characterised by crenulation cleavage in lower grades and pervasive schistosity in higher metamorphic zones.

Ar–Ar whole rock, muscovite and hornblende ages

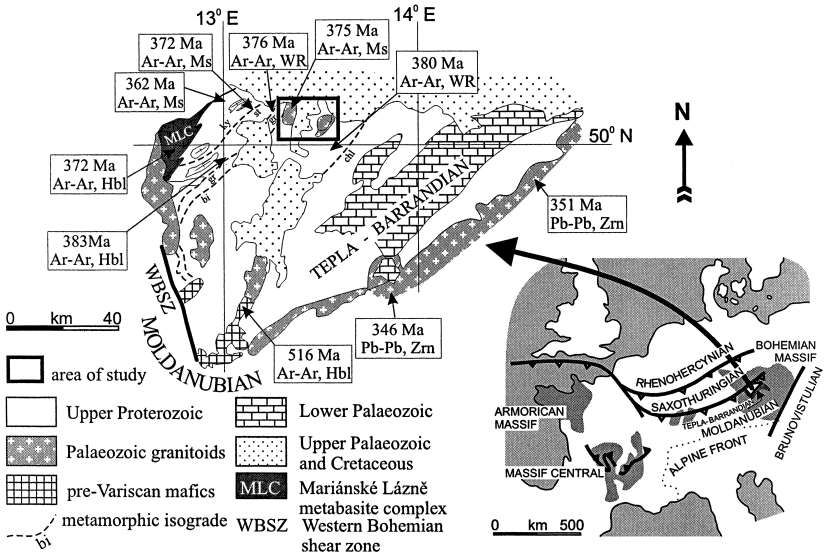

Fig. 1. Geological sketch map of the Teplá-Barrandian zone within the Bohemian Massif and the Variscan orogen in Europe. Radiometric ages of several localities after Dallmeyer and Urban (1994) and Holub et al. (1997), see text for details. Abbreviations: Hbl—hornblende, Ms—muscovite, WR—whole-rock, Zrn—zircon.

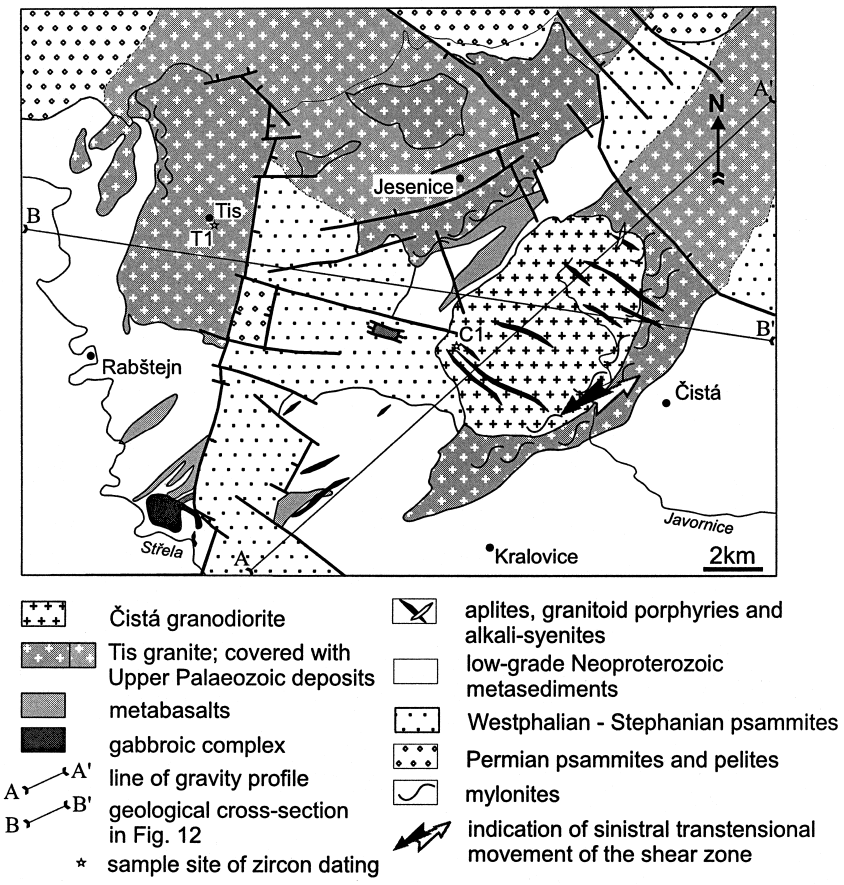

Fig. 2. Schematic geological map of the Čistá granodiorite and the country rocks.

for rocks of the above-mentioned metamorphic zones (Fig. 1) show consistent Devonian cooling ages (Dallmeyer and Urban, 1994; Dallmeyer et al., 1995) which correspond to the termination of sedimentation in the Barrandian Palaeozoic basin (Chlupáč, 1993). In summary, the Teplá–Barrandian rocks were affected by a prograde Barrovian metamorphism during the Middle Devonian, and were associated with a compressive deformation (Zulauf, 1997).

The studied area consists of two types of granitoid marked by a contrasting mode of emplacement at different times: the Tis granite and the Čistá granodiorite stock. The Tis biotite granite outcrops in patches separated at the level of erosion by the Neoproterozoic metasedimentary country rocks and by the transgressive sediments of Permo-Carboniferous grabens (Fig. 2). This large pluton stretches far to the northeast beneath the Carboniferous, Permian and Cretaceous deposits, as evidenced from exploration boreholes. According to the gravity data (Dobeš and Polanský, 1967), the Tis granite body has a thin laccolith shape (Fig. 3). In addition, field observations indicate that the Tis granite laccolith intruded parallel to the Neoproterozoic bedding and prior to the formation of the vertical cleavage of a Devonian age. Ar–Ar dating of muscovite from the Tis granite yielded an age of 375 Ma (Dallmeyer and Urban, 1994). These authors ascribed this age to an early Variscan rejuvenation of

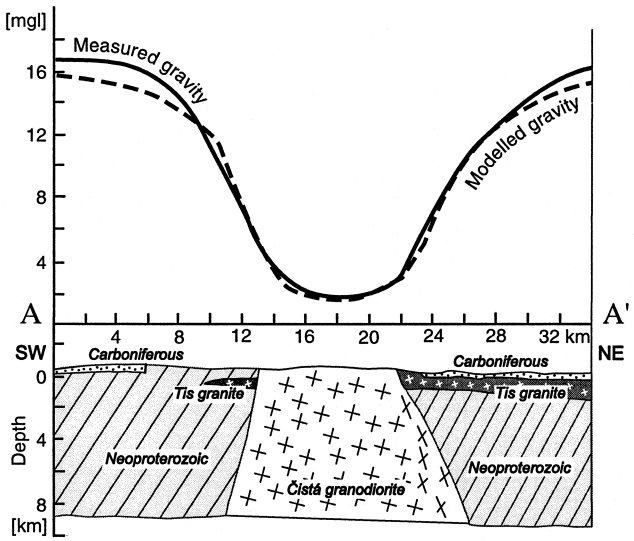

Fig. 3. Gravity data from a profile through the Čistá granodiorite and the country rocks (indicated in Fig. 2) and interpretative geological cross-section (Dobeš and Polanský, 1967).

the argon system that closed during the magmatic cooling at about 500 Ma ago. Similar Ar–Ar ages around 380–376 Ma were also obtained from the surrounding Neoproterozoic metasediment. Re-opening of the Ar–Ar system may be attributed to the ambient Devonian metamorphism in the metasediment surrounding the Tis granite whose grade was high enough (chlorite and biotite zones).

The Čistá granodiorite stock has a roughly elliptical shape (5×3 km^2) in the map view (Fig. 2), with its main axis trending NE–SW. This suggests a vertical and deep-rooted form of the granodiorite stock is derived from the gravity survey (Dobeš and Polanský, 1967). To the west, the Čistá stock intruded directly into the Neoproterozoic rocks. The thermal effect of the Čistá intrusion is confined to a narrow contact aureole comprising hornfels and spotted slate from the Neoproterozoic shales, graywackes and phyllites. To the east, it intruded the Tis type granite; the contact between these two granitoids coincides partly with the NE–SW striking ductile shear zone. The Čistá stock and its surroundings are crosscut by abundant dyke and sill swarms with dominant NW–SE strikes, but few dykes have NNW–SSE and E–W strikes. These dykes are composed of aplites or aplo-pegmatites with zonal structures, granodiorite to quartz–diorite porphyrites and lamprophyres.

2.1. Petrography of the granitoids

The Čistá amphibole–biotite granodiorite consists of two subtypes showing a concentric pattern (Klomínský, 1963; Kopecký et al., 1997). The core of the intrusion is built of medium- to fine-grained biotite granodiorite without any visible preferred orientation. At the periphery, the granodiorite stock is more mafic and exhibits magmatic foliations. An increasing proportion of plagioclase vs. K-feldspar toward the margins documents variations in the composition. The mean modal composition of the granodiorite is plagioclase (An_{15-30}) 50%, K-feldspar 15%, quartz 28%, biotite 5% and hornblende <1%. Plagioclase is euhedral with normal-oscillatory zoning. K-feldspar occurs as microcline or perthitic orthoclase. Quartz is anhedral and undulatory. Euhedral titanite, apatite, zircon, magnetite and muscovite are present as accessories. The Tis biotite granite is a coarse-grained, pale yellow–red rock due to haematitised biotite. The granite has a subhedral granoblastic structure which is random, or sometimes planar along the eastern margin of the intrusion marked by larger amount of muscovite. The modal composition is plagioclase (An_{10-15}) 27%, K-feldspar 37%, quartz 25% and biotite 8% plus accessory muscovite, ilmenite, apatite, and zircon (Klomínský, 1963). K-feldspar mostly occurs as euhedral, up to 1.5-cm crystals.

Table 1
Pb isotopic data from single grain zircon evaporation

Sample number	Zircon colour and morphology	Grain#	Massscans[a]	Evaporation temp. (°C)	Mean $^{207}Pb/^{206}Pb$ ratio[b] and $2\sigma_m$ error	$^{207}Pb/^{206}Pb$ age and 2-σm error
C1	Clear to yellow, long-prismatic idiomorphic	1	108	1597	0.054045 ± 38	372.9 ± 1.6
		2	76	1599	0.054036 ± 46	372.6 ± 2.0
		3	107	1596	0.054040 ± 34	372.7 ± 1.5
		4	93	1601	0.054051 ± 19	373.2 ± 0.8
		5	96	1599	0.054062 ± 18	373.7 ± 0.7
Mean of five grains		1–5	480		0.054047 ± 14	**373.1** ± 1.1[c]
	As above	6	74	1599	0.054526 ± 39	392.8 ± 1.6
T1	Clear to light grey, long-prismatic, slightly rounded terminations	1	118	1599	0.057333 ± 30	504.4 ± 1.2
		2	94	1600	0.057360 ± 25	505.7 ± 1.0
		3	86	1600	0.057348 ± 28	504.9 ± 1.1
		4	99	1596	0.057344 ± 28	504.8 ± 1.1
Mean of four grains		1–4	397		0.057345 ± 14	**504.8** ± 1.0[c]
	As above	5	104	1600	0.061328 ± 42	650.8 ± 1.5

[a] Number of $^{207}Pb/^{206}Pb$ ratios evaluated for age assessment.
[b] Observed mean ratio corrected for nonradiogenic Pb where necessary. Errors based on uncertainties in counting statistics.
[c] Error enhanced to reproducibility of internal standard (for details see Kröner and Hegner, 1998).

3. Zircon geochronology

Single zircons from samples of both the Čistá and Tis plutons were dated by the Pb–Pb evaporation method using the technique developed by Kober (1986, 1987) and modified for use in the Mainz laboratory by Kröner and Todt (1988). The analytical procedures are described in Kröner and Hegner (1998), and the data are presented in Table 1. Errors are at the 2σ (mean) level or correspond to the reproducibility of the Mainz zircon standard (Kröner and Hegner, 1998). Sample C1 from the Čistá granodiorite was collected at the western margin of the stock (Fig. 2), whereas sample T1 from the Tis granite comes from the core of the laccolith (Fig. 2). Both samples represent undeformed rocks.

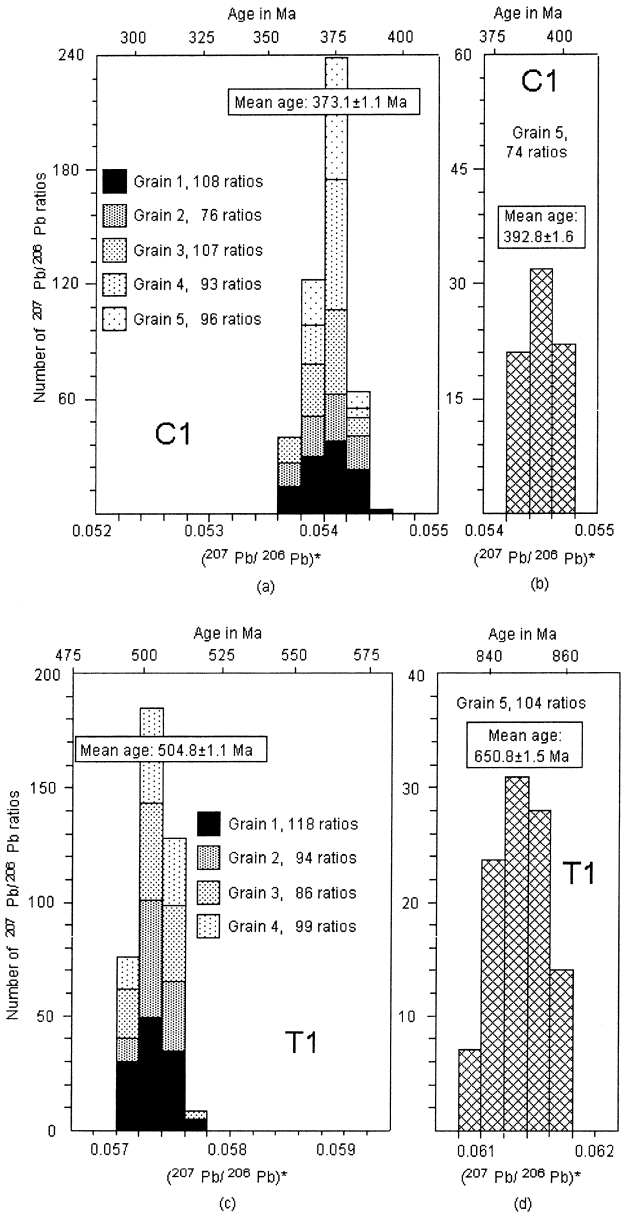

Fig. 4. Histograms showing distribution of radiogenic lead isotope ratios derived from evaporation of single zircons from Čistá and Tis granitoid intrusives, Teplá-Barrandian zone, Bohemian Massif. (a) Spectrum for five grains from Čistá granodiorite sample C1, integrated from 480 ratios and interpreted to reflect time of granodiorite emplacement. (b) Xenocrystic grain. (c) Spectrum for four grains from Tis granite sample T1, integrated from 397 ratios and interpreted to reflect time of granite emplacement. (d) Xenocrystic grain.

Zircons of the Čistá granite are long-prismatic, clear to light yellow–brown, translucent and euhedral, typical of magmatic growth. Core and overgrowth relationships were not observed under the binocular microscope. Six grains were evaporated of which five yielded a mean $^{207}Pb/^{206}Pb$ age of 373.1 ± 1.1 Ma (Table 1, Fig. 4a) that we interpret as reflecting the time of granodiorite emplacement. One grain yielded a slightly older age of 392.8 ± 1.6 Ma (Table 1, Fig. 4b), and we suspect that this is a mixed age between an older core and 373 Ma overgrowth. Since we do not have cathodoluminescence evidence for this assumption we do not ascribe much significance to this age.

Zircons of the Tis granite are yellow–brown to grey–brown, not transparent, and display slight to significant rounding at their terminations that we ascribe to metamorphic recrystallisation. Three grains provided consistent $^{207}Pb/^{206}Pb$ ratios that combine to a mean age of 504.8 ± 1.0 Ma (Table 1, Fig. 4c). One grain shows a significantly older age of 650.8 ± 1.5 Ma (Table 1, Fig. 4d) which we interpret as being a xenocryst derived from Cadomian-age crust below the Tis pluton. This age is similar to zircon ages obtained from the Brunovistulian domain along the northeastern boundary of the Bohemian Massif (Kröner et al., 2000).

4. Structural pattern of the country rocks

To the east of the Čistá granodiorite, the bedding (S_0) of the Neoproterozoic metasediment is sub-horizontal or affected by open buckle folds with NE–SW-trending axes and steep axial planes. The bedding is preserved in psammitic flat-lying layers, otherwise it is mostly overprinted by a low-grade axial planar cleavage (S_1) associated with F_1 folds. This cleavage strikes NE–SW and is formed by the planar alignment of chlorite, muscovite and quartz aggregates. To the east of the Čistá granodiorite, S_1 cleavage dips to the northwest at angles of 20–80°. To the west, along with the increasing metamorphic grade, the folds progressively tighten, S_1 becomes steeper to the NW and S_0 disappears. Whilst the foliation strikes remain constant throughout the entire study area, the westward increase in foliation dip is accompanied with a decrease in plunges of the lineation (Figs. 5 and 6). To the west of the Čistá intrusion, NW and SE dips of S_1

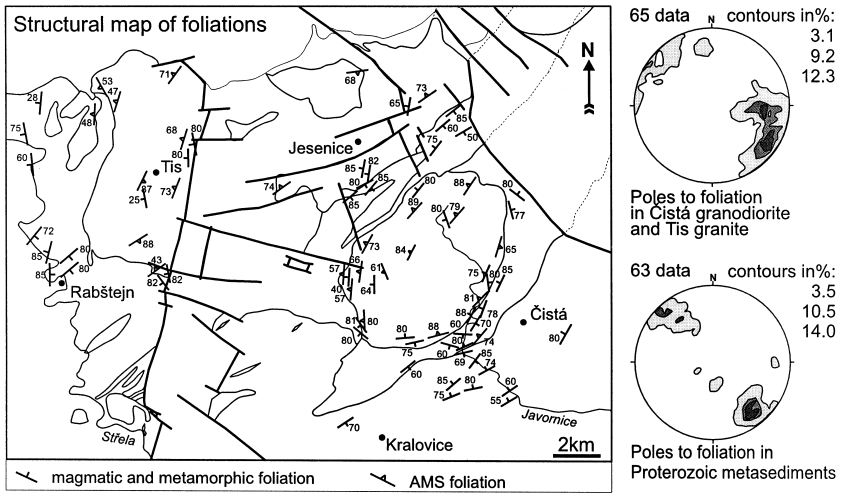

Fig. 5. Structural map of foliations in the Čistá granodiorite and the country rocks.

are observed. This fan-like cleavage pattern is attributed to large-scale NW–SE folds several hundred metres in wavelength (Fediuk, 1994; Holubec, 1995). L_1 NE–SW-trending mineral lineations plunging to the NE or SW at shallow angles (Fig. 6) are defined by chlorite alignments and fine grooving on cleavage planes. The F_1 folds have their axes parallel to the chlorite lineation, i.e. dipping at low angles to the NE or SW. In places where cleavage is most intense, isoclinal rootless folds are observed, centimetres to decimetres in wavelength with asymmetric limbs where shearing is intense. Lenses and segregations of quartz occur along the cleavage planes and also in fold hinges. Regionally, these S_1, L_1 and F_1 are attributed to the NW–SE oriented compression under the greenschist facies metamorphism dated by Ar–Ar (muscovite) at around 380 Ma (Dallmeyer and Urban, 1994).

A subsequent deformation phase D_2 produced sets of kink-bands with centimetre- to several-metre-wide limbs and axial planes dipping to the NW at shallow to medium angles, sometimes to SE depending on S_1 dips (Fig. 7a, b), and kink axes are generally trending NE–SW. This late deformation resulted from bulk vertical shortening and NW–SE stretching under very low-grade metamorphic conditions (Figs. 6 and 8). East of the Čistá granodiorite, this tectonic event produced shear bands (Fig. 7c) indicating a sinistral extensional dip-slip movement. In some places quartz-infilled tension gashes crosscut the cleavage and form asymmetric arrays implying normal faulting towards the NW.

5. Structures and fabrics in the granitoids

The oval Čistá granodiorite stock yields visible magmatic foliations only at its periphery, as defined by flattened mafic enclaves and shape preferred orien-

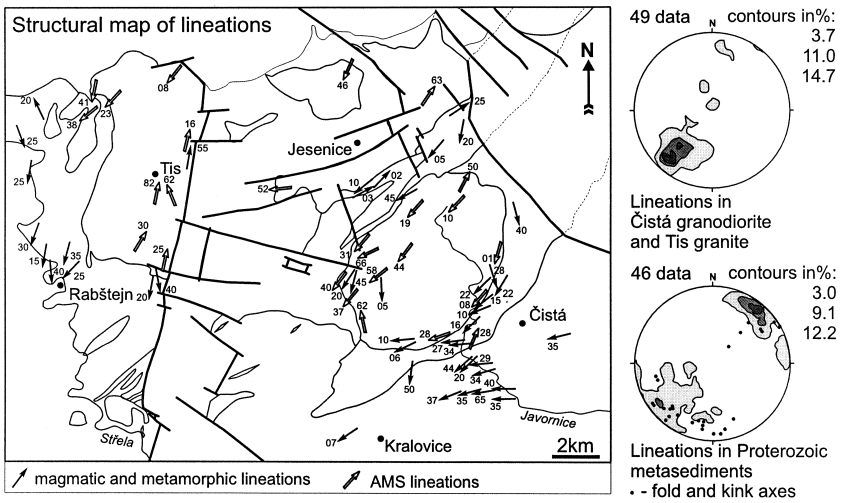

Fig. 6. Structural map of lineations in the Čistá granodiorite and the country rocks.

tations of plagioclase, K-feldspar and biotite. The foliations are parallel to the intrusion margins, especially along its long sides (Fig. 5). At the eastern border of the stock, the magmatic foliation increases in intensity and grades into solid-state mylonitic fabric. In the core of the intrusion the fabric is cryptic and can be defined only by AMS. Linear magmatic structures are defined by long axes of stretched mafic enclaves and by lineations given by flakes of biotite. The major trend of magmatic lineations is NE–SW with plunges 10–40° to the SW (Fig. 6).

Unravelling the structure of the Tis granite is more difficult as the pluton is partly covered with younger sediments forming several isolated outcrops. In the western part of the pluton, the granitic magma interfingered with bedding planes of the Neoproterozoic metasedimentary rocks. Near the contacts, angular fragments of the metasediment and a thin zone of contact metamorphism were found. Macroscopic magmatic fabric is rarely visible and most data come from the AMS study. No post-magmatic ductile deformation was observed except at the eastern margin of the Čistá granodiorite stock, where a west-dipping shear zone occurs. This NE–SW-trending Čistá Shear Zone (CSZ) is 100 m wide and affects, up to mylonite, the eastern border of the Tis granite (see above) with SSW-plunging stretching lineations and top-to-the-SSW oriented movements. Geometry and kinematics of this transtensional shear zone agree with the extensional kink-bands that developed in the Neoproterozoic metasediment (Fig. 8).

5.1. Anisotropy of magnetic susceptibility in the granitoids

The AMS fabric in undeformed igneous rocks

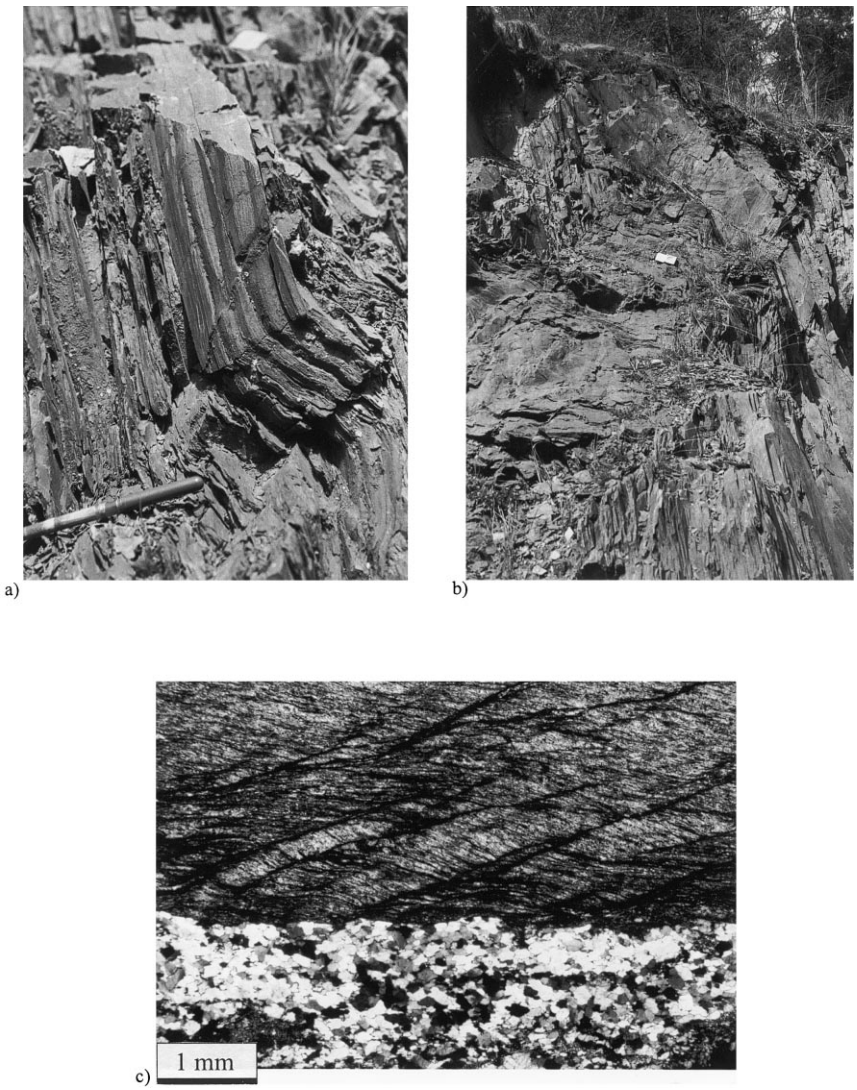

Fig. 7. (a) Kink band in the Neoproterozoic phyllites indicating vertical shortening. (b) Large-scale kink band in the Neoproterozoic phyllites. (c) Shear band in the Neoproterozoic metapelites at contact with a quartz lens.

characterises the magmatic fabric whereas in other rocks the more complex fabric reflects mainly the symmetry and intensity of the solid-state strain. The magnetic fabrics were then used to ascertain the structural data recorded in the field and to complement them in localities where no macroscopic features were observed. In the granodiorite, the magnetic susceptibility is carried dominantly by the accessory ferromagnetic magnetite and paramagnetic biotite and amphibole. In the Tis granite the susceptibility carriers are represented by ferromagnetic haematite and pyrrhotite, and paramagnetic biotite and ilmenite (Chlupáčová et al., 1975). Consequently, mean susceptibilities in the granodiorite are, due to its magnetite content, about two orders of magnitude higher that in the granite.

Two AMS parameters have been used, the degree of anisotropy (P) and ellipsoid shape factor (T) (Jelínek, 1978): $P = k_1/k_3$ and $T = 2(y_2-y_3)/(y_1-y_3)$, where k_1, k_2, k_3 are values of the principal AMS ellipsoid axes with $y_1 = \ln k_1$, $y_2 = \ln k_2$, $y_3 = \ln k_3$.

The degree of anisotropy values vary from 1.02 to 1.7, corresponding to undeformed isotropic granite and mylonitised magnetite-rich granodiorite, respectively. The ellipsoid shape factors vary from $+0.1$ to $+0.9$ in the Čistá granodiorite indicating oblate fabrics, whilst the Tis granite fabric with T values from -1 to $+1$ covers the complete range of prolate to oblate shapes. According to similarities in the AMS characters, the sampled sites were grouped into four areas (Fig. 9): (i) western outcrops of the Tis granite, (ii) shear zone along the eastern margin of the Čistá granodiorite, (iii) central zone of the Čistá granodiorite, and (iv) western margin of the Čistá granodiorite.

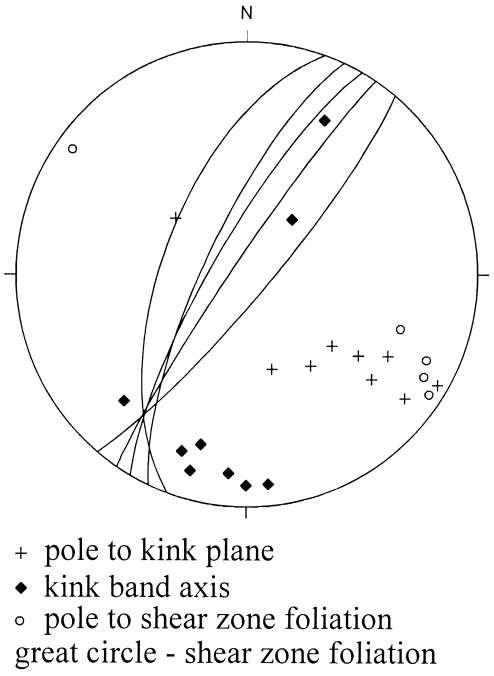

Fig. 8. Stereographic projection of structural elements from the Neoproterozoic rocks and the shear zone.

1. Lack of exposures in the western part of the Tis granite prevents from drawing a complete structural pattern of the pluton. However, some general fabric features can be defined: a very low degree of anisotropy, P = 1.02–1.08 on average, with a scatter smaller than in the granodiorite, contrasting with highly variable symmetries, from strongly prolate to strongly oblate ellipsoid shape, $T = -0.6$–0.7. The magnetic foliations have chiefly NNE–SSW strikes and steep dips to the west. The magnetic lineations dominantly plunge to the NNE at variable angles. The low degree of anisotropy corresponds to invisible magmatic fabric at majority of the sites, however, at the western and northern margin the granite has a clear plane strain to oblate fabric resulting from superimposed solid-state deformation as evidenced by microstructures (see below). At one site (no. 23) in the centre of the pluton, a strong magnetic lineation and weakly defined foliation may have been formed by a constrictional magmatic flow.
2. The eastern margin of the Čistá granodiorite yields a very high degree of anisotropy, up to $P = 1.7$, due to the mylonitisation of the previous magmatic fabric along the CSZ. The degree of anisotropy increases with the strain intensity, and the orientation of the magnetic fabric coincides with the macroscopic structures measured in the field. The shape of magnetic ellipsoid is moderately oblate at all localities ($T = 0.2$–0.5). The magnetic foliation is steep or nearly vertical, striking NNE–SSW in the northern part of the shear zone, and follows the shape of the stock to strike ENE–WSW at its southern end. The foliation dips, either to the NW, or to the SE (Fig. 5), are controlled by the subvertical CSZ. The magnetic lineations plunge gently to the SW (Figs. 6 and 9).
3. In the central zone of the Čistá granodiorite the AMS data represent the only possible information on the igneous fabric. The magnetic fabric has a low degree of anisotropy, $P = 1.1$–1.4, characteristic of the weak alignment of rock-forming particles developed during the magma flow. In spite of this low fabric intensity, all data clearly show an oblate shape of the AMS ellipsoid, up to $T = 0.8$. The magnetic foliation remains parallel to the pluton margins, i.e. NE–SW to NNW–SSE, maintaining steep dips. The magnetic lineations plunge rather steeply, mostly to the SW, except the southern end of the central zone where they dip to the NNW.
4. The western margin of the Čistá granodiorite is

marked by intense magnetic fabric, up to $P = 1.7$. As the magmatic fabric is not overprinted by a subsequent deformation, it suggests that the magma straining along the pluton periphery was larger than in its interior. The T parameter varies from plane strain to oblate ellipsoids, slightly increasing with the anisotropy degree. The foliations are very steep and their strike follows again the shape of the stock, rotating from NE–SW in the north to N–S in the south. The magnetic lineations have intermediate plunges of 30–50°, predominantly to the SW.

Summarising the AMS data on the Čistá granodiorite intrusion, the magnetic foliations show a concentric

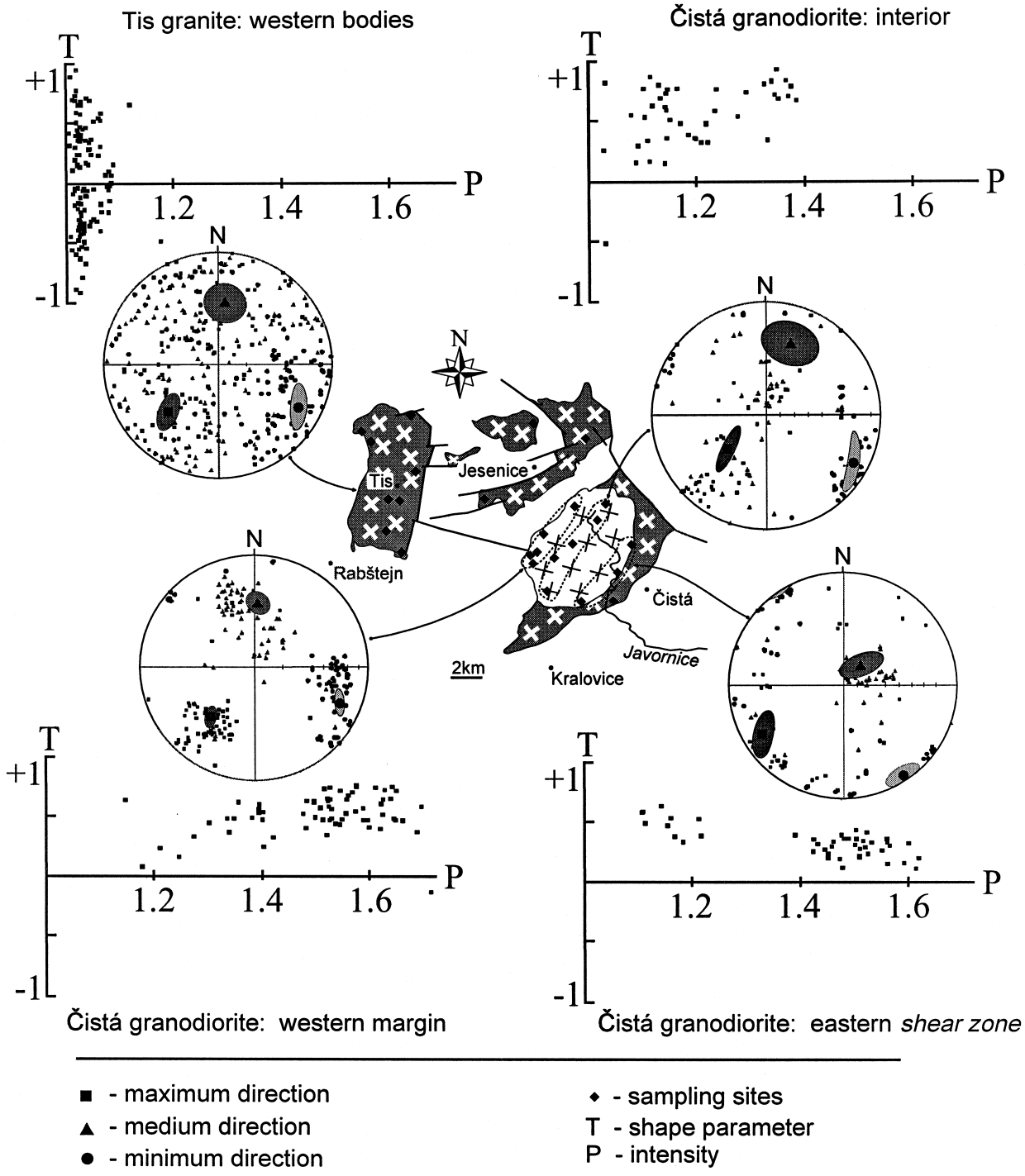

Fig. 9. Anisotropy of magnetic susceptibility data from the Čistá granodiorite and Tis granite. For definition of P and T parameters see the text. Ellipses in stereograms correspond to confidence regions, main directions of AMS are indicated with 95% confidence.

pattern around the periphery, whilst the core zone displays foliations with a regular NE–SW strike and steep dips. Magnetic lineations plunge at shallow angles in the periphery whilst in the central zone they are steep. This overall pattern suggests that the pluton apex, where conventionally presumed flat-lying foliations are preserved, was removed by erosion.

6. Microstructures in the deformed granitoids

The CSZ affected both the Tis granite and the Čistá granodiorite and runs parallel to their contact (Fig. 2). Movements along this shear zone produced a range of deformation structures in these rocks, depending on their former mineral compositions, igneous fabrics and thermal states. In a profile across the shear zone, the strain intensity increases from magmatic fabrics up to ultramylonite in the Čistá granodiorite, and from undeformed granite to mylonite in the adjacent Tis granite. We describe differences in the structural evolution of the rocks during the mylonitisation. Each rock is presented at three stages of deformation from the least to the most deformed.

6.1. Tis granite

The Tis granite is plastically deformed within a zone of 100–700 m along the eastern margin of the Čistá stock. Zones of fine-grained ultramylonite occur locally reaching a thickness of 0.5–2 m.

In the undeformed Tis granite, mostly anhedral perthitic K-feldspars up to 1 cm in size occur. Plagioclase appears as 0.5 cm in size, often euhedral crystals with albite-twin lamellae. Quartz is present in interstices of a skeleton formed by K-feldspar and plagioclase and exhibits a chessboard undulatory extinction. Incipient recrystallisation occurs along boundaries of

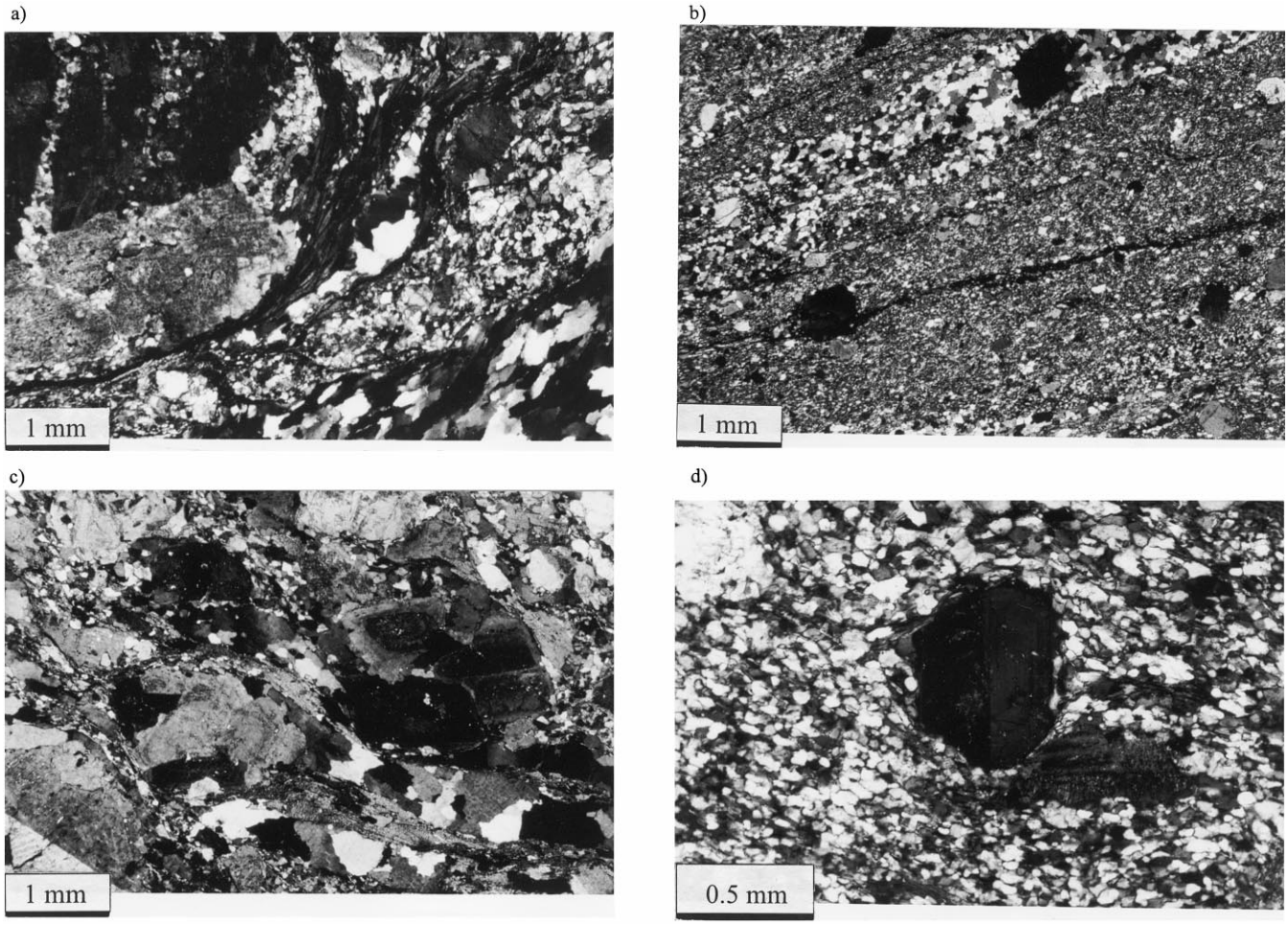

Fig. 10. (a) Mylonite of the Tis granite. Grain-size reduction of recrystallised quartz aggregate is due to an anvil effect of plagioclase phenocryst. Plagioclase is partly transformed into polycrystalline fine-grained aggregates; (b) Banded microstructure (IWL) in the Tis granite ultramylonite with relics of plagioclase phenocrysts; (c) Mylonite of the Čistá granodiorite. Recrystallised quartz forms polycrystalline aggregates and together with fine-grained matrix anastomoses around relics of plagioclase phenocrysts; (d) Ultramylonite of the Čistá granodiorite. Detail of recrystallised matrix containing rounded plagioclase phenocryst.

large subgrains producing thin zones of strain-free minute grains with cuspate–lobate boundaries. Biotite is mostly undeformed or kinked perpendicular to the basal planes.

The medium-deformed Tis granite has a porphyroclastic structure with locally well-developed *C–S* fabrics. K-feldspar appears bookshelved, rotated by shearing and separated by recrystallised quartz, or is locally recrystallised into aggregate neoblasts of 300–400 μm with grain boundaries parallel to the perthitic surfaces. Myrmekitic patches often rim margins of K-feldspars. Plagioclase is partly transformed into polycrystalline fine-grained aggregates with interstitial recrystallised biotite (Fig. 10a). Newly formed grains of 50–100 μm in size are commonly rectangular, sometimes joined in triple junctions. Quartz grains 300–500 μm in size form polycrystalline ribbons. Their boundaries are mostly lobate, sometimes straight, indicating grain boundary migration recrystallisation. Quartz aggregates located in-between the K-feldspar fragments are marked by grain-size reduction suggesting stress concentrations in these areas. Biotite is entirely recrystallised and occasionally displays basal slip which is responsible for mica fish formation.

The mylonite of the Tis granite (Fig. 10b) has a banded structure at the millimetre scale in which complete recrystallisation of quartz forms ribbons alternating with fine-grained layers of biotite and monomineralic layers of recrystallised plagioclase or K-feldspar. Recrystallised K-feldspars, 50–100 μm in size, are irregular in shape. Aggregates of plagioclase consist of recrystallised grains with straight boundaries and well-developed triple junctions. The long faces of new grains are often parallel with small flakes of biotite. Quartz forms monomineralic ribbons composed of recrystallised and irregularly shaped grains 300–500 μm in size. The grains often contain prismatic subgrain boundaries which are oblique to the quartz ribbon boundaries. Leftover grains and cuspate grain boundaries indicate intense grain-boundary migration recrystallisation mechanism. This succession of deformational microstructures is consistent with solid-state deformation of already solidified granite under rather high temperature conditions within a shear zone (Schulmann et al., 1996).

6.2. Čistá granodiorite

The Čistá granodiorite shows a complete transition from plastically undeformed well-developed magmatic fabric, through pre-RCMP (rheological critical melt percentage) transitional fabric, to solid-state ortho gneiss and mylonite along the eastern border of the stock.

The magmatic and pre-RCMP fabrics, ubiquitous in the western and central part of the granodiorite stock, are dominated by zoned, mostly euhedral plagioclase phenocrysts, 3–10 mm across, forming an interconnected framework with a weak shape-preferred orientation. Interstices in the plagioclase skeleton are mostly filled with undeformed biotite, with no preferred orientation and quartz aggregates 0.5–1 mm in size. Some phenocrysts of plagioclase are transected by submagmatic microfractures filled with quartz (Bouchez et al., 1992). Quartz grain-boundaries are lobate to straight, attesting to incipient grain boundary migration. Some displacement of plagioclase boundaries led to the nucleation and growth of new strain-free grains of quartz, up to 100 μm in size. Wide fringes of myrmekite along their boundaries accompany a few K-feldspars.

In the mylonitised granodiorite (Fig. 10c) at the eastern margin, up to 50% of the plagioclase forms recrystallised aggregates or ribbons merging into a fine-grained matrix isolating relics of plagioclase phenocrysts. Biotite is often smeared out and forms anastomosing layers. Quartz appears as polycrystalline aggregates, around 1 mm in mean grain size. Quartz recrystallisation took place by the mechanism of grain-boundary migration as suggested by leftover grain microstructures. Infrequent prismatic subgrain boundaries are oblique to the mylonitic foliation.

Within the rare ultramylonite corridors (Fig. 10d), the recrystallised matrix constitutes more than 90% of the rock and has a uniform 50–100 μm grain size irrespective of the mineral species. Relics of rounded plagioclases, 1–2 mm in size, are scattered in the matrix. Grain boundaries of matrix phases are straight to slightly lobate and parallel to foliation.

6.3. Quartz microfabric

Orientations of about 200 quartz *c*-axes were measured in *XZ* sections (parallel to lineation and normal to foliation) using the universal stage and were plotted on a lower hemisphere, equal area stereonet (Fig. 11). The measurements were taken from the foliated western border of the Čistá granodiorite (K18b, C6/1) and from the zone of ductile deformation affecting the eastern border of the Čistá stock (K31) and adjacent Tis granite (C20/2). In samples K18b and C6/1, weak maxima occur close to foliation and close to the *Y* axis of the finite strain. The other maxima plot along the periphery of diagram, some of them close to lineation direction. Sample K18b shows maxima symmetrically distributed with respect to the *XY* plane, and forming an angle of about 45° with the foliation. The *c*-axis orientation with maximum close to *Y* direction and two maxima at 45° positions to the elongation correspond to type II crossed girdle pattern with high opening angle of 90°, reported from granulite facies rocks (Lister and Dornsiepen, 1982). The

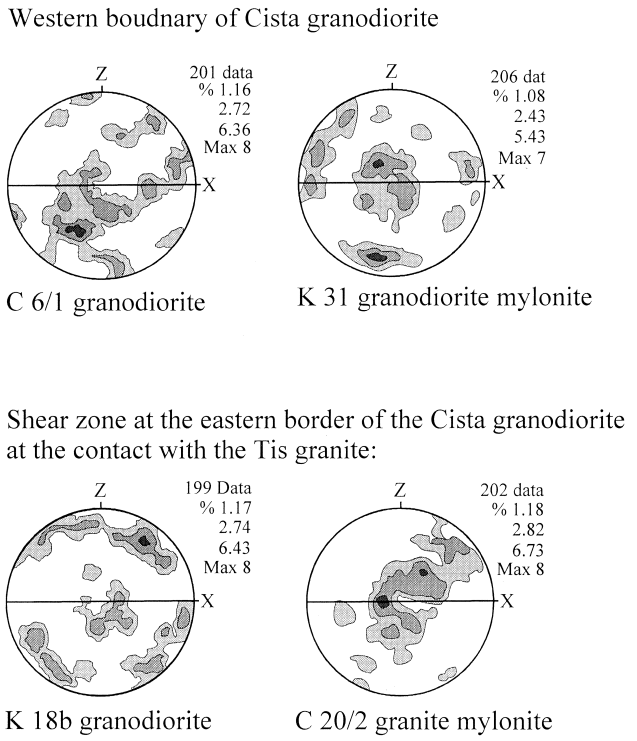

Fig. 11. Quartz *c*-axis fabrics and location of samples from the Čistá granodiorite and Tis granite. Percentages indicate concentrations of axis distribution; projection on lower hemisphere, equal area net.

observed texture pattern and microstructures attest to high activity of prism-[*c*] slip accommodating coaxial deformation commonly reported from granitoids deformed at the solidus boundary (Gapais and Barbarin, 1986).

Mylonitic sample (K31) shows strong maximum near the *Y* axis of finite strain, subordinate maximum close to foliation pole and weak maximum close to lineation. The former two maxima may be interpreted as resulting from combined activity of prism- $< a >$ and basal- $< a >$ slip. The latter maximum close to mineral lineation is commonly attributed to the activity of prism-[*c*] slip. We interpret such a fabric in terms of continuous shear deformation during cooling from high to lower temperatures when the activity of prism-[*c*] is gradually replaced by prism-[*a*] glide. This evolution agrees with the maxima close to *Y* and disappearance of axes in the *X* direction. The quartz *c*-axis pattern within ribbons of banded mylonitic Tis granite exhibits a single girdle oblique to the foliation and lineation (Fig. 11). Principal maxima are distributed between the periphery of diagram and its centre suggesting a combined activity of prism- $< a >$, rhomb- $< a+c >$ and basal- $< a >$ slip. This type of quartz *c*-axis preferred orientation is commonly reported from greenschist to lower amphibolite facies conditions. The asymmetry of quartz fabric in the deformed granitoids suggests a prevalence of non-coaxial deformation, which matches with the strain observations from the field.

7. Interpretation of structural data and numerical modelling

The structural study of the Neoproterozoic host rocks and both the Tis and Čistá granitoids demonstrated the existence of folded Neoproterozoic stratification associated with development of steep regional cleavage. This pattern is in agreement with observations of Zulauf (1997) who attributed it to the NW–SE oriented upper Devonian compressional activity. The compressional deformational event is, however, absent in both the sub-horizontal sheet of the Tis granite and in the Čistá granodiorite stock. The cleavage developed in the Neoproterozoic metasedimentary rocks is affected by subsequent sub-horizontal kink-bands indicating a bulk vertical shortening and NW–SE stretching. This extensional deformation materialises as a narrow ductile shear zone, the CSZ, developed along the eastern border of the Čistá granodiorite and adjacent Tis granite. The geometry and kinematics of this transtensional shear zone are consistent with the extensional kink-bands that developed in the Neoproterozoic metasedimentary rocks (Fig. 12). The internal fabric of the Čistá granodiorite, described by means of the AMS method, reveals steep magnetic foliations and lineations moderately to steeply plunging to the SW in the western and central parts of the stock, respectively. The magnetic lineation becomes flatter approaching the CSZ. The fabric symmetry is generally weakly oblate and the degree of fabric intensity increases from the core of intrusion towards the western and eastern margins of the stock. In contrast, the Tis granite shows very weak fabric intensity and no systematic fabric pattern. These geometric and kinematic data may be interpreted as syntectonic intrusion of the Čistá granodiorite along the transtensional shear zone crosscutting the rigid sheet of the Tis granite. This geometrical model is supported by microstructural and quartz microfabric analyses, which attest that two different sequences of deformation developed in both described granitoids. The Tis granite was deformed once already solidified only within the narrow shear zone in the solid-state and at relatively high temperature. In contrast, the Čistá granodiorite is typical of a syntectonically cooled intrusion. It was deformed whilst incompletely solidified with microstructures spanning from widely developed magmatic to pre-RCMP stages, to the progressively more localised high-temperature solid-state deformation, and finally towards strongly localised ultramylonites.

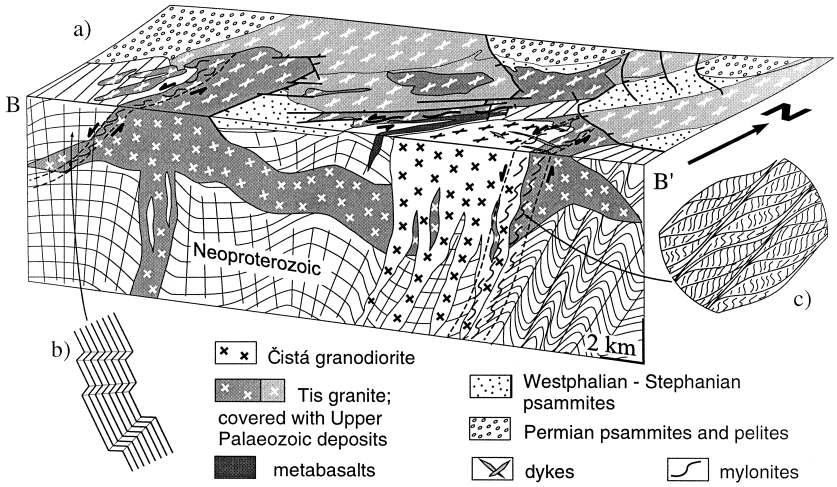

Fig. 12. (a) Schematic cross-section of the Čistá granodiorite area along the line B–B′ depicted in Fig. 2. Shear couples indicate transtensional movement in the shear zone. (b, c) Kink and shear bands attributed to this tectonic regime, yet under different thermal conditions.

Based on the above discussed data, a model of the Čistá granodiorite stock emplacement in general extensional regime is suggested. The Tis granite is seen as a rigid sub-horizontal sheet, which resisted regional compressional Devonian folding and cleavage development in soft host rocks. The regional extension, which affected this steep fabric, also had a small effect on the stiff Tis granite. However, it is only in the area of the Čistá granodiorite intrusion where the extensional shear zone developed consistently with regional tectonic pattern. We suggest that the granodiorite magma (Čistá stock) emplaced beneath the thick and rigid Tis granite sheet. In the area of the ascending Čistá granodiorite, the solid granite of the Tis laccolith may have been locally highly weakened and in combination with regional transtension a ductile fault may have been activated. Hence, we speculate that subsequent batches of magma were able to ascend along this fault into higher levels and solidify as a Čistá stock. Weakening of the Tis granite laccolith is simulated using a numerical model that assesses the thermal, hence rheological, evolution of host rocks in relation to the ascending Čistá granodiorite magma.

7.1. Thermal and rheological evolutions of host rocks during magma ascent and emplacement

In the model it is assumed that the magma ascended in a liquid state through a feeder zone up to the Tis granite laccolith, representing the major rheological boundary where further ascent was blocked and a horizontally elongated secondary magma chamber developed. We have employed the CONTACT program (Peacock, 1989), based on a

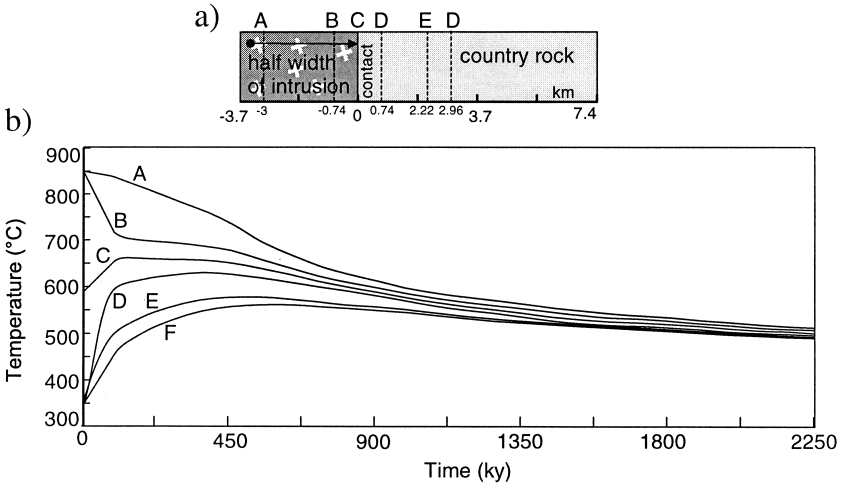

Fig. 13. (a) Scheme of the intrusion setting modelled by program CONTACT (Peacock, 1989). (b) Temperature vs. time plot for points at a different distance from the intrusion, time is counted from the instantaneous intrusion of the granodiorite.

Table 2
Parameters adopted in the thermal model of the granodiorite intrusion

Half width of intrusion	3700	m
Temperature of country rocks	350	°C
Temperature of intrusion	850	°C
Interval of crystallisation	100	°C
Heat of crystallisation	200	kJ kg^{-1}
Thermal conductivity	2.51	W m^{-1} K^{-1}
Heat capacity	1000	J kg^{-1} K^{-1}
Density	2800	kg m^{-3}

finite-difference algorithm solving a one-dimensional heat transfer equation (Carslaw and Jaeger, 1959). This program simulates the thermal adjustment between an instantaneously emplaced two-dimensional intrusion and its country rocks (Fig. 13a). The input parameters are listed in Table 2. A temperature of 350°C is considered suitable for the country rocks as they belong to the chlorite and biotite metamorphic zones. The granodiorite intrusion temperature is set at 850°C, the interval of crystallisation at 100°C, and the approximated half-width of the stock at 3700 m according to its present size. We assume that this distance may represent a rough estimate of the size of the secondary magma chamber developed below the rigid and horizontally elongated obstacle. In our model the thermal solution is calculated for a horizontally elongated chamber in a vertical direction. The resulting temperatures at various distances from the intrusion and with time during cooling are given in Fig. 13(b). It indicates that the periphery of the intrusion (point −0.74 km) cooled to the solidus (750°C) in less than 220 ka whilst the core of the intrusion (point −3 km) was still partially molten (temperatures above 750°C) as long as 450 ka. Temperatures in the country rocks reached their maximum values between 450 and 540 ka before joining the cooling trend of the intrusion.

Table 3
Parameters in stress calculations

	Quartzite (wet)	Albite granite	Quartz–diorite
A ($Pa^{-n}s^{-1}$)	2.0×10^3	1.3×10^6	2.0×10^4
E (kJ mol^{-1})	154	234	219
β	0.75	0.75	0.75
N	2.3	3.9	2.4

The resulting temperatures were used to calculate a strength profile of the crust with a relatively hot geotherm. This geotherm (Fig. 14a), assessed to fit pressure–temperature data of the Devonian metamorphism in the Barrandian (Zulauf, 1997), is based on the assumption that the Barrandian zone corresponded in the Devonian times to a rigid cover on top of an orogenic root built of hot lower and middle crustal rocks (Zulauf, 1997). The corresponding lithological column is approximated as follows: the lower crust is composed of 35 km of quartz–diorite, and the upper crust of 35 km of quartzite. The Tis laccolith represents a horizontal slab between 17 and 20 km deep, estimated from the metamorphic conditions of the host rocks.

The strength (σ_b) was calculated using Byerlee's con-

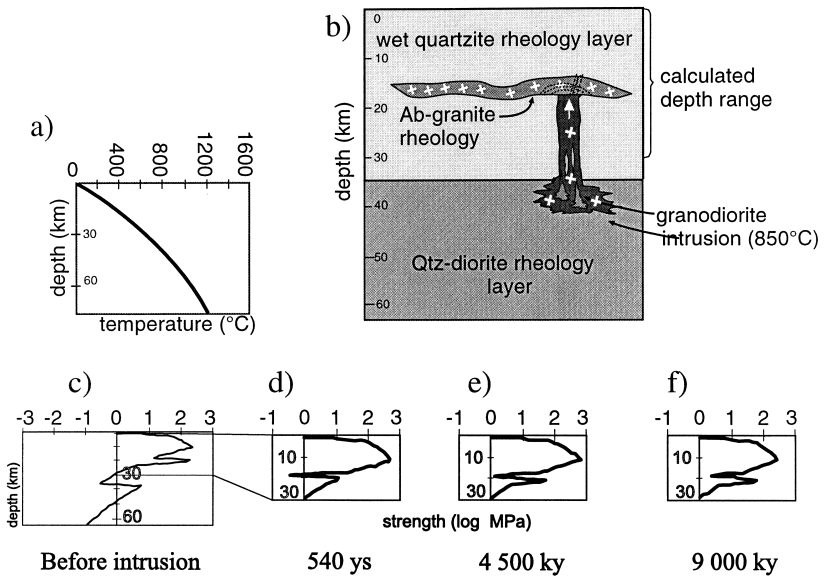

Fig. 14. (a) Geotherm for the Teplá–Barrandian zone estimated using pressure–temperature data of Zulauf (1997). (b) Schematic model of crustal stratification of the Teplá–Barrandian zone used for rheological calculations. (c–f) Strength profiles of the modelled crust at different times after the intrusion of granodiorite.

stants for the brittle crust (see Ranalli and Murphy, 1987):

$$\sigma_b = \beta\rho g(1-\lambda)z \quad (1)$$

where β is a parameter depending on the type of faulting ($\beta = 0.75$ for extension), ρ is the density, g is the gravitational acceleration, λ is the pore fluid factor ($\lambda = 0.36$), and z is the depth.

To calculate the strength (σ_v) of the viscous crust the power-law creep was used:

$$\sigma_v = (e/A)^{1/n} \exp(Q/nRT) \quad (2)$$

where e is the strain rate, A, n and Q are material constants. Q corresponds to activation energy for creep, n is the power law exponent, R is the gas constant and T the absolute temperature. The values of the chosen parameters and material constants are listed in Table 3. Rheological parameters for different parts of the crustal column are after Jaoul et al. (1984) for the quartzitic crust, Ranalli and Murphy (1987) for quartz–diorite of the lower crust, and Shalton and Tullis (1981) for the Tis granite and albitic granite.

In the model, the ascending granodiorite magma (Čistá stock) is instantaneously emplaced at a depth of 20 km beneath the 3-km-thick, rigid laccolith formed by the Tis granite (Fig. 14b). Before the intrusion of the Čistá stock, the rheological stratification already exhibits a decreasing resistance in the viscous part of the quartzitic upper crust perturbed by a yield strength maximum of the Tis granite layer (Fig. 14c). After intrusion of the Čistá granodiorite, the crustal strength profile evolves due to the input of heat (Fig. 14d–f). The maximum thermal perturbation is reached in ca. 540 ka after intrusion: a temperature of ca. 500°C was achieved up to a distance of 3 km from the roof of the intrusion along with a strong decrease in yield strength of the overlying granitic laccolith which became as plastic as the quartz–diorite at depths of >30 km (Fig. 14d). The final diagram at 900 ka (Fig. 14f) shows that, at that time, the crust recovered the strength close to the original steady state.

7.2. Rheological and microstructural evolutions of the granitoids after emplacement of the Čistá granodiorite

Along with the assumption that the Čistá granodiorite was emplaced during an extensional event, we therefore assume that the rest of granodiorite was emplaced along an extensional shear zone following the failure of the thermally weakened Tis granite sheet. We now examine the thermal and rheological evolutions of both the Čistá granodiorite and the Tis granite during subsequent cooling.

Immediately after necking and failure of the Tis granite sheet, a granodiorite magma began to fill the neck zone within which no shear stress was further transmitted to the solid host rocks. We believe that ductile deformation of the host rocks could have started again after the granodiorite itself became solid allowing shear stress transfer to its surroundings. This could have occurred when the temperature of the granodiorite became lower than its solidus (~750°C), i.e. ~400 ka after its emplacement.

At this stage the Čistá and Tis granitoids can be viewed as a polyphase mineralogical system consisting dominantly of K-feldspar and quartz. Handy (1990, 1994) applied a concept of strain and stress concentrations related to deformation of polyphase materials. According to this concept, the rocks form two types of structures: (1) Load-bearing framework (LBF) in which the stress is concentrated in strong phases surrounding pockets of weak material, and (2) Interconnected weak layers (IWL) marked by concentration of stress and deformation in weak minerals forming an interconnected framework. As indicated by experiments, progressive deformation leads to breakdown of LBF structure which is highly unstable under higher strains (Jordan, 1987). It gives rise to the so-called 'banded structure' marked by alternation of monomineralic layers. In granitic rocks this structure develops when one strong (K-feldspar) and two weak phases of different viscosity (plagioclase stronger than quartz) occur (Schulmann et al., 1996). However, Martelat et al. (1999) has shown that in exceptionally hot quartz–feldspar tectonites (granulites of Madagascar) with a high proportion of weak quartz (30%) the LBF structure is not a transient microstructure and does not collapse into a more stable IWL structure. This structure is developed in rocks with two rheologically contrasting phases, strong feldspar and weak quartz (Martelat et al., 1999).

We interpret the medium deformed Tis granite as forming a LBF structure formed by strongest K-feldspar 37% and weaker oligoclase 27%, whilst weakest quartz 25% and biotite 8% are forming isolated pockets. Banded ultramylonite is interpreted as forming IWL structures with a low viscosity contrast between the strong and weak fractions (Handy, 1994; Schulmann et al., 1996). The mylonites developed in the Čistá granodiorite along the CSZ are characterised by persistence of LBF, consisting of weak quartz aggregates (25%), with no interconnection even under substantial strain, and of a skeleton formed by strong calcic plagioclase and K-feldspar (up to 70%). However, the weak fraction increases in volume with increasing strain due to recrystallisation of plagioclase in a similar manner as described by Martelat et al. (1999). The rheological evolution of the LBF structure of the Čistá granodiorite and the LBF and IWL structures of the Tis granite are now modelled. The bulk strength of the LBF structure is estimated using the

Eudier–Tharp formula (Eudier, 1962; Tharp, 1983), modified for recrystallised peridotites by Rutter and Brodie (1988) and for granulite tectonites by Martelat et al. (1999):

$$\sigma_{\text{rock}}^{\text{LBF}} = (1-K\varphi_{\text{w}}^{2/3})(\sigma_{\text{feldspar}}-\sigma_{\text{quartz}}) + \sigma_{\text{quartz}} \quad (3)$$

where σ_{rock} is the strength of the porous aggregate, φ_{w} is the volume proportion of the weak phase, and K is an experimental factor depending on the pore shape, taken as $K = 1.8$ (Tharp, 1983; Rutter and Brodie, 1988; Handy, 1990).

The bulk strength of the IWL structure is given by Handy (1994):

$$\sigma_{\text{rock}}^{\text{IWL}} = \sigma_{\text{quartz}}\varphi_{\text{quartz}}^{(1-x)} + \sigma_{\text{feldspar}}(1-\varphi_{\text{quartz}})^{-1}(1-\varphi_{\text{quartz}}^{1-x}) \quad (4)$$

where

$$x = 1-\varphi_{\text{quartz}}/\varphi_{\text{feldspar}}.$$

The bulk strength estimates (Fig. 15) were calculated in the Tis granite at 0.74 km and 2.98 km from the contact, and in the Čistá granodiorite at 0.74 km from the contact. Eq. (3) for the LBF structure was used for strength calculations in the case of the Čistá granodiorite and the Tis granite in a distance of about 3 km from the contact, where this rock is only weakly deformed. Eq. (4) for the IWL structure was used for the Tis granite close to the contact.

The results (Fig. 15) indicate that, away from the contact (~3 km), the Tis granite is always stronger than the Čistá granodiorite. However, its strength decreases significantly during heating before its convergence toward the strength of the Čistá granodiorite during the cooling. Near the contact, the Tis granite with its IWL structure decreases in strength during 500 ka. Then its strength becomes equal or even weaker than that of the adjacent Čistá granodiorite. These strength relationships explain why the localised shear zone affected the rigid granite sheet, and support the assumption that both the eastern margin of the Čistá granodiorite and the adjacent Tis granite experienced solid-state deformation approximately at the same time.

8. Conclusion

The Pb–Pb evaporation on zircons yields ages of the Čistá granodiorite and Tis granite of 373 Ma and 504 Ma, respectively. The structural approach combined with thermal and mechanical modelling illustrates that the emplacement of the Čistá granodiorite occurred during a transtensional event documented in the granitoids and the Neoproterozoic metasediments of the study area. The granodiorite magma rapidly ascended through dykes intruding the lower to middle crust and formed a stock (Fig. 12a). The width of the stock was probably growing during the sinistral transtensional motion of the shear zone. The observed transition from the magmatic fabrics to the solid-state mylonitic foliations is likely to have resulted from the syntectonic intrusion followed by continuous shearing after the emplacement.

The Caledonian granitic laccolith represented a major rheological obstacle in the ascent of the magma. The Neoproterozoic rocks show distributed low-grade extensional deformation whilst the granitic laccolith is affected merely by a ductile shear zone. This contrast in the deformation pattern is explained by thermal weakening of the granite sheet caused by the ascending

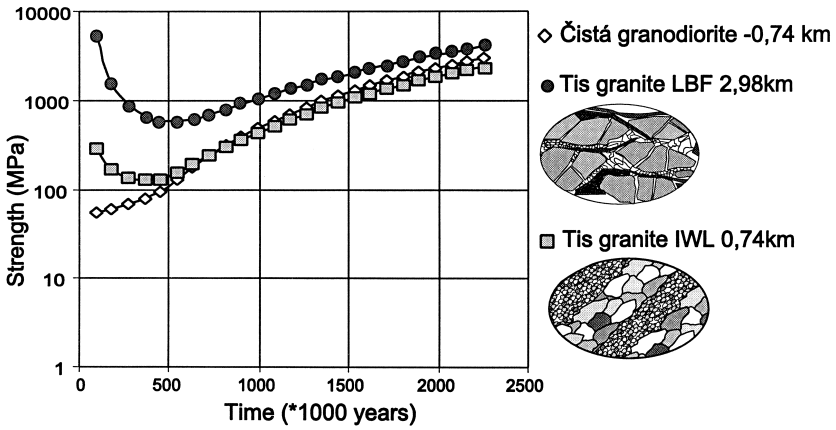

Fig. 15. Evolution of modelled rock strength at different places of the pluton. The Tis granite near the contact with intruding Čistá granodiorite has an IWL microstructure and its strength approaches values of the Čistá granodiorite soon after the intrusion. On the contrary, farther from the contact, the granite mylonite characterised by a LBF microstructure is temporarily weakened but its strength is always greater than that of the Čistá granodiorite.

granodiorite leading to failure of otherwise rigid granitic rocks.

The southwestern direction and shallow plunge of magnetic lineations in the sheared granodiorite in conjunction with sinistral movement indicators therefore testify to the transtensional mode of the magma emplacement. The AMS study combined with the microstructural analysis showed a geometrical coherence between the cryptic magmatic and visible solid-state fabrics in the Čistá stock. The intensity of the AMS increases towards the transtensional shear zone together with rotation of the magnetic lineation from a subvertical to subhorizontal plunge (Fig. 9). This structural pattern is interpreted as a vertical magmatic ascent overprinted along the margins of the stock by sinistral transtensional movements during progressive solidification. The AMS study of the Tis laccolith shows a very weak fabric with varying orientation. The only site with strong solid-state fabric geometrically coherent with the solid-state fabric in the Čistá stock occurs along the adjacent shear zone. The thermal modelling, though only one-dimensional, gives a reasonable first-order estimate of thermal and rheological states following the magma intrusion. Heating of the granite, due to the granodiorite ascent, led to thermal softening and development of this high-temperature ductile shear zone several hundred metres thick. Moreover, the modelled results show that the granite near the contact with the granodiorite is thermally so weakened that its yield strength becomes equal, or even weaker than that of the emplaced granodiorite.

Acknowledgements

We highly appreciated thoughtful reviews by Jean-Luc Bouchez and Jean-Louis Vigneresse. Support by the Grant Agency of Charles University (grant #247/96/B-GEO to Z. Venera), the Czech National Grant Agency (grant #205/98/K004) and the Ministry of Education (grant #2431 3005) are acknowledged. We thank František Hrouda (AGICO, Brno) for processing our AMS samples and sharing a part of his AMS data. We are grateful to Josef Jezek for preparing a spreadsheet for geotherm and strength profile calculations, and to Pavel Pitra, Jan Košler and David Dolejš for their valuable comments. We wish to remember our friend Radek Melka who had been present at the beginning of this project but passed away before it was finished.

References

Bouchez, J.-L., Delas, C., Gleizes, G., Nédélec, A., Cuney, M., 1992. Submagmatic microfractures in granites. Geology 20, 35–38.

Brun, J.-P., Pons, J., 1981. Strain patterns of pluton emplacement in a crust undergoing non-coaxial deformation, Sierra Morena, Southern Spain. Journal of Structural Geology 3, 219–230.

Carslaw, H.S., Jaeger, J.C., 1959. Conduction of Heat in Solids. Oxford University Press, New York.

Cháb, J., Suchý, V., Vejnar, Z., 1995. Tepla-Barrandian Zone (Bohemicum): Metamorphic evolution (VII.B.4). In: Dallmeyer, R.D., Franke, W., Weber, K. (Eds.), Pre-Permian Geology of Central and Eastern Europe. Springer-Verlag, Berlin, pp. 404–410.

Cháb, J., Žáček, V., 1994. Metamorphism of the Teplá crystalline complex. KTB Report 3, 33–37.

Chlupáč, I., 1993. Geology of the Barrandian (A Field Trip Guide). Senckenbergische Naturforschende Gesellschaft-Verlag Waldemar Kramer, Frankfurt am Main.

Chlupáčová, M., Hrouda, F., Janák, J., Rejl, L., 1975. The Fabric, genesis and relative age relations of the granitic rocks of the Čistá–Jesenice massif. Gerlands Beiträge Geophysik 84, 487–500.

Dallmeyer, R.D., Franke, W., Weber, K., 1995. Pre-Permian Geology of Central and Eastern Europe. Springer-Verlag, Berlin.

Dallmeyer, R.D., Urban, M., 1994. Variscan vs. Cadomian tectonothermal evolution within the Teplá–Barrandian zone, Bohemian Massif, Czech Republic: evidence from $^{40}Ar/^{39}Ar$ mineral and whole rock slate/phyllite ages. Journal of the Czech Geological Society 39, 21–22.

Dobeš, M., Polanský, J., 1967. Kladensko-rakovnická pánev. Prehodnocení geofyzikálních prací. Geofyzika, n.p, Praha.

Dudek, A., Fediuk, F., 1955. Zur Altersfrage der Metamorphose im barrandienischen Proterozoikum. Geologie 4, 397–403.

Eudier, M., 1962. The mechanical properties of sintered low-alloy steels. Powder Metallurgy 9, 278–290.

Fediuk, F., 1994. Planární prvky proterozoika sv. obruby cisteckojesenického masivu (Planar elements in the Proterozoic of the NE rim of the Čistá-Jesenice Massif). Věstník CGÚ 69, 93–95.

Gapais, D., Barbarin, B., 1986. Quartz fabric transition in a cooling syntectonic granite (Hermitage massif, France). Tectonophysics 125, 357–370.

Handy, M., 1990. The solid-state flow of polymineralic rocks. Journal of Geophysical Research 95, 8647–8661.

Handy, M., 1994. Flow laws for rocks containing two non-linear viscous phases: a phenomenological approach. Journal of Structural Geology 16, 287–301.

Holub, F.V., Cocherie, A., Rossi, P., 1997. Radiometric dating of granitic rocks from the Central Bohemian Plutonic Complex (Czech Republic): constraints on the chronology of thermal and tectonic events along Moldanubian–Barrondian boundary. Comptes Rendeus de l'Academie de Science 325, 19–26.

Holubec, J., 1973. Assyntische Strukturen im Barrandium der Böhmischen Masse. Veröffentlichungen des Zentralinstituts für Physik der Erde 14, 411–415.

Holubec, J., 1995. Tepla-Barrandian Zone (Bohemicum): Structure (VII.B.2). In: Dallmeyer, R.D., Franke, W., Weber, K. (Eds.), Pre-Permian Geology of Central and Eastern Europe. Springer-Verlag, Berlin, pp. 392–397.

Jaoul, O., Tullis, J., Kronenberg, A., 1984. The effect of varying water content on the behaviour of Heavitree quartzite. Journal of Geophysical Research 89, 4298–4312.

Jelínek, V., 1978. Statistical processing of anisotropy of magnetic susceptibility measured on groups of specimens. Studia geophysica et geodetica 22, 50–62.

Jordan, P.G., 1987. The deformational behavior of bimineralic limestone–halite aggregates. Tectonophysics 135, 185–197.

Klomínský, J., 1963. Geologie Cisteckého masívu. Sborník geologických věd G 3, 7–26.

Kober, B., 1986. Whole-grain evaporation for $^{207}Pb/^{206}Pb$-age-investigations on single zircons using a double-filament thermal ion source. Contributions to Mineralogy and Petrology 93, 482–490.

Kober, B., 1987. Single-zircon evaporation combined with Pb^+ emitter-bedding for $^{207}Pb/^{206}Pb$-age investigations using thermal ion mass spectrometry, and implications to zirconology. Contributions to Mineralogy and Petrology 96, 63–71.

Kopecký, L.j., Chlupáčová, M., Klomínský, J., Sokol, A., 1997. The Čistá–Jesenice pluton in western Bohemia: Geochemistry, geology, petrophysics and ore potential. Sborník geologických věd LGM 31, 97–127.

Kröner, A., Todt, W., 1988. Single zircon dating constraining the maximum age of the Barberton greenstone belt, southern Africa. Journal of Geophysical Research 93, 15329–15337.

Kröner, A., Hegner, E., 1998. Geochemistry, single zircon ages and Sm–Nd systematics of granitoid rocks from the Góry Sowie (Owl) Mts., Polish West Sudetes: evidence for early Palaeozoic arc-related plutonism. Journal of the Geological Society of London 155, 711–724.

Kröner, A., Štípská, P., Schulmann, K., Jaeckel, P. (2000). Chronological constraints on the pre-Variscan evolution of the northeastern margin of the Bohemian Massif, Czech Republic. In: Orogenic processes—quantification and modelling in the Variscan belt of central Europe. Franke, W., Altherr, R., Haak, V., Oncken, O., Tanner, D. (Eds.). Special Publication, Geological Society of London, in press.

Lister, G.S., Dornsiepen, U.F., 1982. Fabric transition in the Saxony granulite terrain. Journal of Structural Geology 4, 81–92.

Martelat, J.-E., Schulmann, K., Lardeaux, J.-M., Nicollet, C., 1999. Granulite facies microstructures in shear zones of southern Madagascar. Journal of Structural Geology 21, 671–687.

Peacock, S.M., 1989. Thermal modeling of metamorphic pressure–temperature paths: a forward approach. In: Spear, F.S., Peacock, S.M. (Eds.), Metamorphic pressure–temperature paths, 7. American Geophysical Union, pp. 57–102.

Ranalli, G., Murphy, D.C., 1987. Rheological stratification of the lithosphere. Tectonophysics 132, 281–295.

Rutter, E.H., Brodie, K.H., 1988. The role of tectonic grain size reduction in the rheological stratification of the lithosphere. Geologische Rundschau 77, 295–308.

Schulmann, K., Mlčoch, B., Melka, R., 1996. High temperature microstructures and rheology of deformed granite, Erzgebirge, Bohemian Massif. Journal of Structural Geology 18, 719–733.

Shalton, G., Tullis, J., 1981. Experimental flow laws for crustal rocks. EOS, Transactions of American Geophysical Union 62, 369.

Tharp, T.M., 1983. Analogies between the high-temperature deformation of polyphase rocks and the mechanical behavior of porous powder metal. Tectonophysics 96, T1–T11.

Vigneresse, J.L., 1995a. Control of granite emplacement by regional deformation. Tectonophysics 249, 173–186.

Vigneresse, J.L., 1995b. Far- and near-field deformation and granite emplacement. Geodinamica Acta 8, 211–227.

Zulauf, G., 1997. From very low-grade to eclogite-facies metamorphism: Tilted crustal sections as a consequence of Cadomian and Variscan orogeny in the Teplá Barrandian unit (Bohemian Massif). E. Schweizerbart'sche, Verlagsbuchhandlung, Stuttgart.